arXiv:1609.09391v1 [cond-mat.mtrl-sci] 29 Sep 2016

Tuning the caloric response of $BaTiO_3$ by tensile epitaxial strain

Anna Grünebohm*
Faculty of Physics and CENIDE, University of Duisburg-Essen, 47048 Duisburg, Germany

Madhura Marathe and Claude Ederer
Materials Theory, ETH Zürich, 8093 Zürich, Switzerland

We investigate the effect of epitaxial strain on the electrocaloric effect (ECE) in $BaTiO_3$ by means of *ab initio* based molecular dynamics simulations. We show that tensile strain can be used to optimize the operation range for ferroic cooling. Strain in the range of $\leq 1\,\%$ can be used to shift the operation temperature by several hundreds of Kelvin both to higher and lower temperatures, depending on the direction of the external field. In addition, the transformation between multi-domain and mono-domain states, induced by an in-plane electric field, results in an additional peak of the adiabatic temperature change at lower temperatures, and a broad temperature interval where the caloric response scales linearly with the applied field strength, even up to very high fields.

1. INTRODUCTION

Within a ferroic material, a variation of the ferroic order parameter can be induced through application of the corresponding conjugate field. Depending on the thermal boundary conditions, this results in an isothermal entropy or an adiabatic temperature change. For example, if an externally applied conjugate field is removed under adiabatic conditions, order parameter and temperature typically decrease. It has been shown that "giant" caloric effects occur for different classes of materials in the vicinity of field-induced structural-ferroic transitions[1,2]. For example, in ferroelectric $BaTiO_3$ (BTO), the largest field-induced change of the order parameter (electric polarization, P), and thus the largest adiabatic temperature change, is observed for temperatures slightly above the transition between the cubic paraelectric high temperature phase and the tetragonal ferroelectric phase at about 400 K[3,4]. Systems that exhibit such giant caloric effects have a huge potential for the development of novel cooling concepts[5–7]. For the case of the electro-caloric effect (ECE)[6,8], much work is focused on thin films[2,3,6,8,9], as the magnitude of the ECE generally increases with the strength of the applied electric field[10], and large fields can be induced by moderate voltages within thin films[9]. In addition, the high surface to volume ratio allows for a fast heat transfer to the environment and thus, potentially, for fast cycling of a device. Thin films also allow to combine the advantages of single crystals (well defined crystallographic orientation) and poly-crystals (mechanical stability during cycling).

Furthermore, thin films are often subject to strain, which can strongly affect the ferroelectric properties, and thus provides an efficient way for tailoring the desired functional properties[11]. If a material such as BTO is grown epitaxially on a surface representing a square lattice, a biaxial strain, η, is imposed along the two in-plane directions (a and b), whereas the lattice constant along the film normal (c) can adjust freely. As a result, the ferroelectric transition temperatures and the relative stability of different ferroelectric phases of BTO are modified, as depicted in fig. 1[12–17]. For zero strain, *i.e.* pure clamping by the substrate, both in-plane and out-of-plane components of the polarization appear at the same transition temperature T_C, equal to the bulk transition temperature. Tensile (positive) strain then increases the transition temperature for the in-plane components of P (*i.e.*, along a and/or b) and decreases the transition tempera-

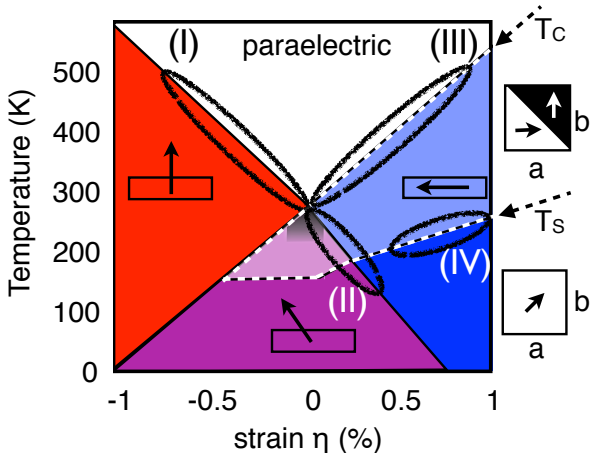

FIG. 1: Schematic phase diagram of $BaTiO_3$ under epitaxial strain, adapted from[17]. Colors encode different polarization (P) directions (also illustrated by the insets). Red: P along c; light blue: a/b multi-domain state (P as sketched on the upper right-hand side); darker blue: ab mono-domain state (P as sketched on the lower right-hand side); light purple: ac/bc domains (in plane P as for a/b domains with homogenous P along c); darker purple: abc mono-domain phase. White dotted lines border multi-domain phases. T_C (T_S) indicates the strain-dependent transition temperature for in-plane P (for the multi-domain to mono-domain transition). The grey area below the bulk T_C for $\eta \approx 0$ indicates a region with complex multi domain states.

*Electronic address: anna@thp.uni-due.de

ture for the out-of-plane component (along c), and vice versa for compressive strain[12,15]. In addition to the ferroelectric mono-domain phases found at low temperatures, multi-domain configurations are stabilized between T_C and T_S[14,16–19].

Generally, a field-induced change of polarization and a resulting adiabatic temperature change occur for all values of strain and all temperatures. However, the largest effect is usually observed just above T_C. This can be understood from the following relation (cf. ref.[6]):

$$\Delta T = -\int_{E_1}^{E_2} \frac{T}{C_E(T,E)} \left.\frac{\partial P}{\partial T}\right|_E dE \quad . \qquad (1)$$

Here, the electric field E is varied from E_1 to E_2 under adiabatic conditions, P is the polarization component along the field direction, and C_E is the specific heat at constant field (and constant pressure). The largest changes, $\partial P/\partial T < 0$, occur just above T_C (where the field causes a transition or crossover to the ferroelectric phase), resulting in a strong peak of $\Delta T(T)$ with a relatively sharp drop on the low temperature side and a broad shoulder towards higher temperatures, see *e.g.* refs.[2,6].

Most previous studies investigating the influence of epitaxial strain on the ECE in BTO have concentrated on compressive strain[20–23]. In contrast, the influence of tensile strain has so far only been investigated based on phenomenological models, with partly contradicting results. For example, both an increasing[20] and a decreasing[21,22] maximal temperature change have been reported. Such discrepancies, which can be caused by different model assumptions or parameterizations, can be resolved through *ab initio*-based simulations. Furthermore, for both kinds of strain we are only aware of investigations on the role of an electric field along the surface normal. However, the ECE in single crystals can depend strongly on the direction of the applied field[24–26]. In addition, the ECE in the multi-domain states with a/b and ac/bc domains and in particular at the corresponding multi-domain to mono-domain transitions at T_S, has not been investigated so far.

In this paper, we address the following questions: Does tensile strain enable or hamper a large caloric response? In particular, can such strain help to obtain a significant ECE over a broad temperature range around ambient temperatures, which is desirable for many applications? How does the strain-induced multi-domain state affect the ECE? To understand these issues, we explore the role of tensile strain on the caloric response of BTO, using *ab initio*-based simulations and taking different directions of the applied field into account. We show that tensile strain $\leq 1\,\%$ can be used to shift $T_{\max}$ by several hundreds of Kelvin both to higher and lower temperatures, depending on the direction of the external field. In addition, the transformation between multi-domain and mono-domain states, induced by an in-plane electric field, results in an additional peak of $\Delta T(T)$ at lower temperatures, and a broad temperature interval where the caloric response scales linearly with the applied field strength, even up to very high fields.

2. METHODS

Molecular dynamics simulations are performed, employing an effective Hamiltonian[27] as implemented in the FERAM code developed by Nishimatsu *et al.*[28].[36] The *ab initio*-based parametrization of the effective Hamiltonian for BTO is taken from ref.[29]. Periodic boundary conditions and a cell size of 96×96×96 BTO units have been used. We model the epitaxial strain imposed through a hypothetical substrate by fixing the elements η_1 ($\equiv \eta_a$) and η_2 ($\equiv \eta_b$) of the homogenous strain tensor (in standard Voigt notation) to the external strain η and setting $\eta_6 = 0$. We define zero strain for a lattice constant of 3.996 Å, which we obtain for the paraelectric phase of bulk BTO directly above T_C.

We note that, due to the large size of our simulation cell, we obtain additional domain configurations, with local polarization along various crystallographic directions, for very small strain values ($|\eta| < 0.1\%$) directly below T_C (see grey area in fig. 1). These configurations are absent for the smaller simulation cell used in ref.[17]. Since these additional domain configurations appear only in a very limited region within the phase diagram they are not relevant in the context of the present study and are therefore not discussed any further.

The caloric response is obtained from the following protocol: (I) We start our simulations above T_C and equilibrate the system within an external field. Afterwards, we reduce the temperature in steps of maximal 10 K, using the final configuration from the previous temperature step as initial configuration, *i.e.* we field-cool the system. These simulations are performed in the NPT ensemble using a Nosé-Poincaré thermostat and a time step of $\Delta t = 2$ fs[30]. (II) At each measuring temperature we start from the corresponding field-cooled configuration, switch to the micro-canonical (NPE) ensemble and perform *direct* simulations of the ECE. Advantages and technical details of this method are discussed in refs.[31–33]. We ramp down the field with the rate of 0.002 kV/cm/fs. This ramping rate is sufficiently slow to ensure thermodynamic equilibrium except very close to the ferroelectric phase transition, where the dynamic of the system slows down considerably. We thus use further equilibration of at least 40 ps previous to measuring the adiabatic temperature change.

We note that the simplifications necessary to construct the effective Hamiltonian lead to quantitative deviations of the calculated ferroelectric transition temperatures (T_C) compared to experiment[27,29]. Nevertheless, qualitative trends and the overall magnitude of polarization and strain are well described and are generally in good agreement with experimental observations, cf. refs.[15,17]. Furthermore, only 3 out of of 15 degrees of freedom per BTO unit are explicitly taken into account in our simu-

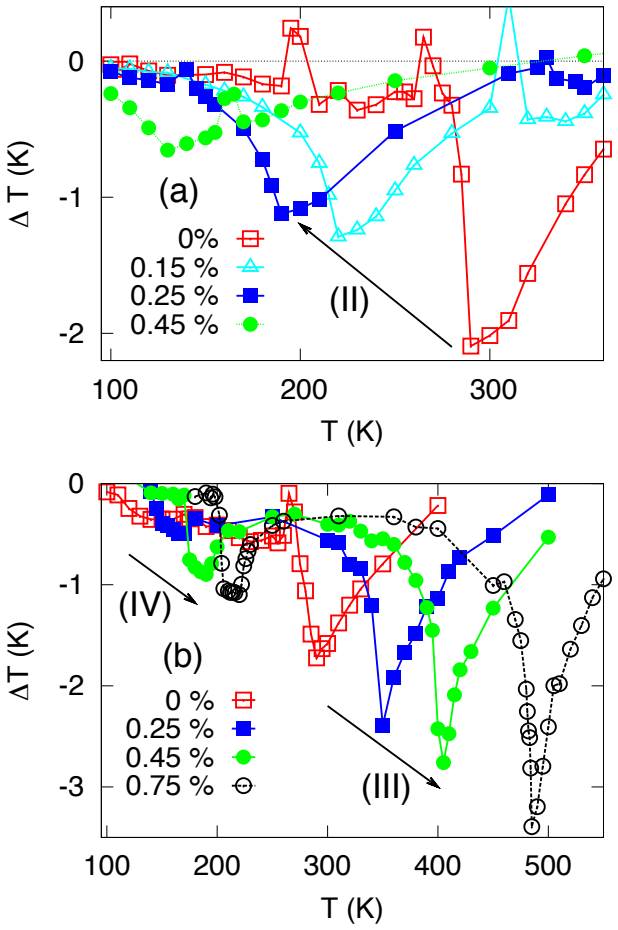

FIG. 2: Adiabatic temperature change of BTO if an external field of 100 kV/cm is removed for different values of tensile strain. a): Field along c; b): field along ab. Arrows illustrate the changes of $T_{\max}$ and $\Delta T(T_{\max})$ with strain in the vicinity of the three transition lines marked (II)-(IV) in fig. 1.

lations, resulting in a reduced specific heat, and thus an overestimated temperature change ΔT. In the following, we therefore rescale the calculated ΔT by a factor of 1/5, according to the ratio between the considered and total number of degrees of freedom, cf. refs.[32,34].

3. RESULTS

Figure 2 shows the calculated electro-caloric temperature change as function of the initial temperature under removal of an electric field of 100 kV/cm applied along the out-of-plane and in-plane directions for different amounts of tensile strain.

We first discuss the case of zero applied strain, $\eta = 0$, *i.e.*, pure clamping, for both field directions. As already discussed in refs.[20,23] clamping reduces the ECE and results in a broadening of the ΔT-peak. For the field along the surface normal we find a reduction by a factor of two compared to the free bulk system (from about 4 to 2 K for an external field of 100 kV/cm) and the full width at half maximum (FWHM) increases from about 35 K (unclamped) to about 55 K (clamped). If the field is applied along the in-plane ab direction, the peak value of the ECE, $\Delta T(T_{\max})$, is reduced to about 1.7 K at $T_{\max} = 290$ K, while the FWHM increases to about 70 K. Thus, in spite of the reduction compared to the free bulk case, a large ECE is still obtained for the clamped system for both field directions.

We note that we find small temperature and field regions where $\partial P/\partial T|_E > 0$, *e.g.* at the transition temperatures of the ferroelectric phase polarized perpendicular to the external field. As a consequence, the adiabatic cooling in these temperature regions is reduced and even an inverse ECE, *i.e.*, a heating of the system under field removal occurs, cf. eq. (1). For instance, at the transition temperature of the in-plane polarization, $T_C \approx 270$ K, for field along c, ΔT changes its sign. In addition, an inverse ($\Delta T > 0$) peak exists around $T \approx 190$ K, the transition temperature to a different multi-domain configuration observed for $\eta \approx 0$. The magnitude of these inverse peaks may be underestimated due to the used temperature grid and as several (meta-) stable domain configurations seem to coexist.

Focusing next on the strain dependence of $\Delta T(T)$, depicted in fig. 2, one can observe that increasing tensile strain shifts the position of the peak in ΔT, $T_{\max}$, towards higher (lower) temperatures if the electric field is applied in-plane (out-of-plane). Thus, the peak positions essentially follow the transition lines (II) and (III) in fig. 1 for the appearance of spontaneous polarization along the respective field direction. Furthermore, with decreasing (increasing) $T_{\max}$, the FWHM of the ECE peak increases (decreases). For example, for a field along c the FWHM increases approximately linearly with strain from about 55 K to about 90 K between 0 and 0.45 % while the FWHM for a field along ab is about 50 K for 0.25–0.45 % and is reduced to 40 K for 0.75% strain.

Most strikingly, the maximum of the ECE, $|\Delta T(T_{\max})|$, increases (decreases) systematically, if the corresponding peak position is shifted to higher (lower) temperatures. This relationship between $|\Delta T(T_{\max})|$ and $T_{\max}$ for different strains can be understood from eq. 1. Even though all quantities under the integral in eq. 1 depend on temperature (and of course on the electric field), we find that the change of the peak value of ΔT under strain is dominated by the explicit factor T in the integrand. This is analogous to what has been found in ref.[23] for BTO under compressive strain and electric field along c, see the corresponding transition line (I) in fig. 1, using the same microscopic model as used in the present work.

The same trend, *i.e.* increasing $|\Delta T(T_{\max})|$ with increasing $T_{\max}$, due to the strain-induced shift in the ferroelectric transition temperature, has also been found in[21] using a modified transverse Ising model and in[22] using phenomenological Landau theory. In contrast,

ref.[20], also using Landau theory, has reported the opposite trend, namely decreasing $|\Delta T(T_{\max})|$ with increasing $T_{\max}$ (and thus increasing $|\Delta T(T_{\max})|$ under increasing tensile strain). The increase of $|\Delta T|$ found in ref.[20] was attributed to a stronger first order character, and thus increasing $\partial P/\partial T|_E$, under tensile strain, cf. eq. 1. This can neither be confirmed by our *ab initio*-based microscopic model nor by the phenomenological models used in[21,22]. We note that, while the Landau free energy in[20] is expanded up to sixth order in the polarization, with temperature-dependent second and fourth order coefficients, ref.[22] uses a different parameterization based on an eighth-order expansion with a temperature-independent fourth order coefficient.

In addition to the main peak at $T_{\max}$, corresponding to the ferroelectric transition temperature of the polarization component along the field direction, for small values of tensile strain and field along c we also observe a small feature in ΔT at the in-plane transition temperature $T_C^{ab} > 300\,\mathrm{K}$. Here, the onset of the in-plane polarization results in a reduced magnitude (or even reversed sign) of ΔT, related to regions with negative $\partial P_c/\partial T|_E$. We note that this is analogous to the "double-peak structure" reported in[22] for tensile strains smaller than 0.15 %. With increasing strain, the magnitude of the "peak" at higher temperatures decreases as T_C^c and T_C^{ab} move apart, see fig. 1.

Summarizing the results presented so far, we point out that epitaxial strain can be used to systematically increase or decrease the temperature range with large ECE over several hundreds of Kelvin for rather moderate strain values of less than 1 %, depending also on the direction of the applied field. In fact, for many of the anticipated device applications, it is important to reduce $T_{\max}$ to ambient temperatures (and also to obtain a sufficiently large ΔT over a broad temperature interval around $T_{\max}$). Here, we find $T_{\max}$ about 100 K below the bulk T_{C}, and thus in a very attractive temperature range for applications, for only 0.25% tensile strain (see fig. 2a).

Next, we discuss the ECE for the multi-domain state observed under tensile strain in the temperature range between T_{C} and T_{S}. As can be seen in fig. 2b for an electric field applied along ab, a second peak in $\Delta T(T)$ is found near the strain-dependent transition temperature T_{S}, indicated as (IV) in fig. 2. The appearance of this peak can be explained as follows. Below T_{S}, the system is in a mono-domain state with a large polarization that depends only weakly on temperature and field. Consequently the system exhibits only a very weak ECE below T_{S}. If an external field along ab is applied, T_{S} shifts to higher temperatures, *e.g.*, for 0.75% strain, T_{S} increases from 185 K (no field) to 220 K (100 kV/cm) to 370 K (500 kV/cm). Therefore, if the external field is increased starting from an initial temperature slightly above T_{S}, the system transforms reversibly from a multi-domain to a mono-domain state. Since the net polarization along ab in the multi-domain a/b state is smaller than in the mono-domain ab phase, the polarization is strongly field- and temperature-dependent around this transition, resulting in a pronounced peak in ΔT.

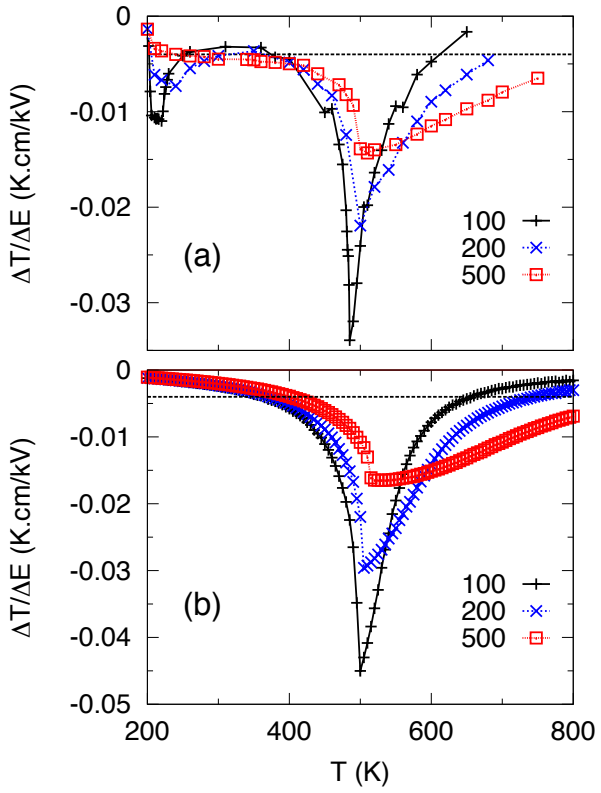

FIG. 3: Electro-caloric strength $\Delta T/\Delta E$ for BTO under $\pm 0.75\,\%$ tensile (a) and compressive (b) strain for electric fields applied along ab (a) and along c (b). Dotted horizontal lines mark an electro-caloric strength of $-0.004\,\mathrm{K{\cdot}cm/kV}$.

While for $\eta = 0$ the corresponding peak value $\Delta T(T^S_{\max})$ for an external field of 100 kV/cm is less than 0.5 K, $\Delta T(T^S_{\max})$ increases with increasing tensile strain and becomes larger than 1 K for 0.75 % strain at about 75 K below the zero-strain T_{C}, see fig. 2 (b). This increase of $\Delta T(T^S_{\max})$ is again related to the corresponding increase of $T^S_{\max}$ via eq. 1, as discussed above for the main ECE peak.

Apart from the additional peak in ΔT, we also observe a moderately large ECE (~ 0.5 K for 0.75 % strain) within a rather broad temperature interval between the two main ECE peaks, namely in the temperature range between T_{S} and T_{C} corresponding to the strain-induced multi-domain configuration. While the corresponding ΔT is small compared to the peak values, it is noticeably larger than within the ferroelectric mono-domain phase below T_{S}. This enhanced ECE is due to the field-induced (and temperature-dependent) gradual rotation of the local polarization from a/b towards ab. Furthermore, as we show in the following, the ECE in this multi-domain region can be considerably enhanced by increasing the field strength.

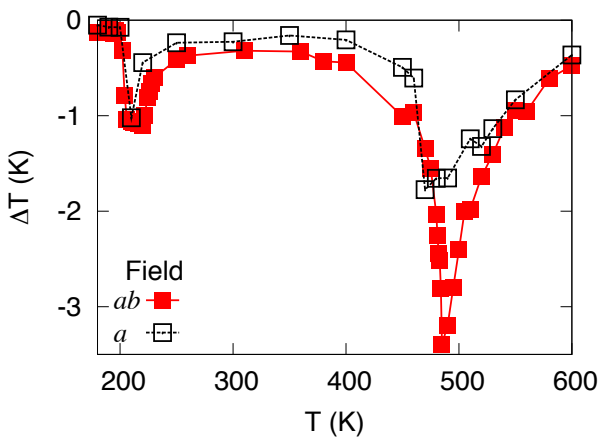

FIG. 4: Adiabatic temperature change of BTO at 0.75% tensile strain under removal of an external field of 100 kV/cm along the a (open black squares) and ab (filled red squares) directions.

Figure 3 shows the "electro-caloric strength", defined as $\Delta T/\Delta E^2$, both under compressive and tensile strain for different applied fields. It can be seen that in both cases the electro-caloric strength decreases near $T_{\max}$ while it increases for even higher temperatures as the field increases. For lower temperatures, which are most relevant for practical cooling applications, the electro-caloric strength under compressive strain is very small and decreases further with the field strength. In contrast, the electro-caloric strength under tensile strain is approximately constant between T_C and T_S, around $-0.004\,\mathrm{K{\cdot}cm/kV}$, even for field strengths up to 500 kV/cm. Thus, between T_C and T_S the ECE grows linearly with the field, and already for a field strength of 200 kV/cm an adiabatic response of 1 K can be obtained in a very broad temperature interval below T_C. For 0.75% strain, this large and broad response occurs about 100 K below the bulk T_C, *i.e.* corresponding to ambient temperatures.

Up to now, the in-plane electric field in our calculations was always oriented along the ab direction. However, we note that even for a misaligned field, a rather strong ECE near T_S is obtained. For example, for an in-plane field along a, we find a similar $\Delta T(T)$ profile and a similar ECE peak at T_S as for the case with the field along ab, see fig. 4. Only the magnitude of the ECE between T_C and T_S and close to the peak at T_C are reduced. This reduced ΔT for E along a is most likely due to the polarization-strain coupling, which does not allow the polarization to rotate fully into the field direction, due to the epitaxial constraint.

Finally, we note that we use "poled" (field-cooled) starting configurations in our simulations, and therefore our results do not include irreversible contributions which can arise in the first field cycle, depending on the thermal history and field treatment of the samples. This can occur due to the existence of different meta-stable multi-domain states, specifically for fields applied along a and $\eta \to 0$.

4. CONCLUSIONS AND OUTLOOK

In summary, we have investigated the effect of epitaxial strain on the caloric response of BTO through *ab initio*-based molecular dynamics simulations. We have focused on tensile strain, which provides a very promising route to enhance the ECE at room temperature and below. With increasing tensile strain, the ECE is systematically reduced for fields along the surface normal. However, since the optimal operation temperature is shifted towards ambient temperatures, small values of tensile strain can be useful in order to optimize the ECE at ambient temperatures. In addition, the ECE peak broadens with increasing tensile strain, which is also favorable for applications.

For an electrical field applied within the surface plane, the ECE exhibits two peaks, one slightly above the ferroelectric transition temperature, T_C, and one close to the transition temperature T_S between the mono-domain and multi-domain ferroelectric phases. Although, the latter is smaller than the peak at T_C, it occurs in a temperature range that is very attractive for many applications. Furthermore, T_S can be adjusted with the magnitude of the strain. Between the strain-dependent temperatures T_S and T_C, we find a reversible coupling between external field and the domain configuration. This strong coupling allows for a linear increase of the ECE with the strength of the external field, and thus large adiabatic temperature changes can be obtained within a broad temperature range. Thus, tensile epitaxial strain can be used to enhance the caloric response of BTO well below the ferroelectric transition temperature, and a considerable ECE around and below room temperature can be achieved if the external electrical field is applied within the surface plane.

Recently, it has been pointed out that the electric field control of the domain structure in BTO can improve the caloric response of FeRh films grown on BTO[35]. Our results suggest that the caloric response of the BTO domain structure itself should also be taken into account, and that the resulting multicaloric properties can be further optimized through epitaxial strain. In the same spirit, one could also consider to use piezoelectric, magnetostrictive, or mechanically-bendable substrates to adjust the caloric response of BTO by shifting its optimal operation range to higher and lower temperatures, which then allows to adjust the cooling device to a specific heat source.

Acknowledgments

We acknowledge financial support by the Deutsche Forschungsgemeinschaft and the Swiss National Science

Foundation (SPP 1599). Anna Grünebohm thanks the Center for Computational Science and Simulation (University of Duisburg-Essen) for computational time.

[1] A. Planes, L. Mañosa, and M. Acet, J. Phys.: Condens. Matter **21**, 233201 (2009).
[2] X. Moya, S. Kar-Narayan, and N. D. Mathur, Nat. Mater. **22**, 439, (2014).
[3] Y. Bai, G.-P. Zheng K. D. Zheng, K. Ding, L. Qiao, S. Q. Shi, and D. Guo, J. App. Phys. **110**, 094103 (2011).
[4] X. Moya, E. Stern-Taulats, S. Crossley, D. González-Alonso, S. Kar-Narayan, A. Planes, L. Mañosa, and N. D. Mathur, Adv. Mater. **25**, 1360 (2013).
[5] S. Fähler, U. K. Rößler, O. Kastner, J. Eckert, G. Eggeler, H. Emmerich, P. Entel, S. Müller, E. Quandt and K. Albe Adv. Eng. Mater., **14**, 10, (2012).
[6] M. Valant, Prog. Mater. Sci. **57**, 980 (2012).
[7] I. Takeuchi and K. Sandeman, Physics Today **68**, 48 (2015).
[8] J. F. Scott, Annu. Rev. Mater. Res. **41**, 229 (2011).
[9] A. S. Mischenko, Q. Zhang, J. F. Scott, R. W. Whatmore, R. W., and N. D. Mathur, Science **311**, 1270 (2006).
[10] S. Lisenkov and I. Ponomareva, Phys. Rev. B **80**, 140102(R) (2009).
[11] D. G. Schlom, L.-Q. Chen, C.-B. Eom, K. M. Rabe, S. K. Streiffer, and J.-M. Triscone, Ann. Rev. Mater. Research **37**, 589 (2007).
[12] N. A. Pertsev, A. G. Zembilgotov, and A. K. Tagantsev, Phys. Rev. Lett. **80**, 1988 (1998).
[13] N. A. Pertsev and V. G. Koukhar, Phys. Rev. Lett. **84**, 3722 (2000).
[14] N. A. Pertsev, V. G. Koukhar, R. Waser, and S. Hoffmann, Integrated Ferroelectrics **32**, 235 (2001).
[15] O. Diéguez, S. Tinte, A. Antons, C. Bungaro, J. B. Neaton, K. M. Rabe, and D. Vanderbilt, Phys. Rev. B **69**, 212101 (2004).
[16] Y. L. Li and L. Q. Chen, Appl. Phys. Lett. **88**, 072905 (2006).
[17] A. Grünebohm, M. Marathe, and C. Ederer, Appl. Phys. Lett. **107**, 102901 (2015).
[18] L. Qiao and X. Bi, Appl. Phys. Lett. **92**, 062912 (2008).
[19] A. S. Everhardt, S. Matzen, N. Domingo, G. Catalan, and B. Noheda, Adv. Electron. Mater. **2015**, 1500214 (2015).
[20] G. Akcay, S. P. Alpa, G. A. Rossetti, and J. F. Scott, J. Appl. Phys. **103**, 024104 (2008).
[21] H.-X. Cao and Z.-Y. Li, J. Appl. Phys. **106**, 094104 (2009).
[22] X. Zhang, J. B. Wang, B. Li, X. L. Zhong, X. J. Lou, and Y. C. Zhou, J. Appl. Phys. **109**, 126102 (2011).
[23] M. Marathe and C. Ederer, App. Phys. Lett. **104**, 212902 (2014).
[24] J. Peräntie, J. Hagberg, A. Uusimäki, and H. Jantunen, Phys. Rev. B, **82**, 134119 (2010).
[25] I. Ponomareva and S. Lisenkov, Phys. Rev. Lett., **108**, 167604 (2012).
[26] F. Le Goupil, A.-K. Axelsson, L. J. Dunne, M. Valant, G. Manos, T. Lukasiewicz, J. Dec, A. Berenov, and N. McN. Alford, Adv. Energy Mater. **4**, 130688 (2014).
[27] W. Zhong, D. Vanderbilt, and K. M. Rabe, Phys. Rev. B **52**, 6301 (1995).
[28] T. Nishimatsu, U. V. Waghmare, Y. Kawazoe, and D. Vanderbilt, Phys. Rev. B **78**, 104104 (2008).
[29] T. Nishimatsu, M. Iwamoto, Y. Kawazoe, and U. V. Waghmare, Phys Rev B **82**, 134106 (2010).
[30] S. D. Bond, B. J. Leimkuhler, and B. B. Laird, Journal of Computational Physics **151**, 114 (1999).
[31] M. Marathe, A. Grünebohm, T. Nishimatsu, P. Entel, and C. Ederer, Phys. Rev. B **93**, 054110 (2016).
[32] T. Nishimatsu, J. A. Barr, and S. P. Beckman, J. Phys. Soc. Jpn. **82**, 114605 (2013).
[33] Y. Liu, J. F. Scott, and B. Dkhil, Appl. Phys. Rev. **3**, 031102 (2016).
[34] A. Grünebohm and T. Nishimatsu, Phys. Rev. B. **93**, 134101 (2016).
[35] Y. Liu, L. C. Phillips, R. Mattana, M. Bibes, A. Barthélémy, and B. Dkhil, Nat. Commun. **7**, 11614 (2016).
[36] `http://loto.sourceforge.net/feram/`